UC San Diego

UC San Diego Electronic Theses and Dissertations

Title

The Complete Mechanism of Chalcone Formation

Permalink

https://escholarship.org/uc/item/0t65x4dd

Author

Chang, Kuei-Lin

Publication Date

2015

Peer reviewed|Thesis/dissertation

eScholarship.org

Powered by the California Digital Library
University of California

UNIVERSITY OF CALIFORNIA, SAN DIEGO

The Complete Mechanism of Chalcone Formation

A thesis submitted in partial satisfaction of the
requirements for the degree Master of Science

in

Chemistry

by

Kuei-Lin Chang

Committee in charge:
Charles L. Perrin, Chair
Joseph M. O'Connor
Robert Pomeroy

2015

Copyright

Kuei-Lin Chang, 2015

All rights reserved.

The thesis of Kuei-Lin Chang is approved, and it is acceptable in quality and form for publication on microfilm and electronically:

Chair

University of California, San Diego

2015

DEDICATION

I would like to dedicate this thesis to my parents for their love and support.

TABLE OF CONTENTS

LIST OF FIGURES

LIST OF SCHEMES

LIST OF TABLES

ACKNOWLEDGEMENTS

I would first like to express my appreciation to Dr. Charles L. Perrin for giving me the opportunity to join his lab. He patiently guides me through this project with his experience and knowledge. Dr. Perrin really helped me a lot on troubleshooting the experiments and interpreting the results. He really cares about his students and wants them to succeed in life. I develop my passion towards research during the time I spent in his lab.

I am grateful to my committee members: Dr. Robert Pomeroy and Dr. Joseph M. O'Connor for their time. I would like to thank Dr. Robert Pomeroy for letting me use the UV spectrophotometers in his lab to complete my research. When problem with the instruments aroused, he was always willing to help me troubleshoot and provide useful alternatives. Dr. Pomeroy also provided me the opportunity to learn many useful analytical instruments that can help me on my research and later in career. I would also like to thank Dr. Joseph M. O'Connor for giving me feedbacks about my research in weekly group meetings. I am grateful for Dr. Gabriel J. Reyes-Rodriguez and Dr. Katie D. Burke for their support in Perrin Group. They have taught me the techniques I need to perform my research in lab and assisted me on all kinds of things during my graduate life at UCSD. Lastly, I would like to thank my parents for supporting me financially and mentally through out my education, and my wife who has encouraged and motivated me while I worked towards this graduate degree.

This research was supported by NSF Grant CHE11-48992.

ABSTRACT OF THE THESIS

The Complete Mechanism of Chalcone Formation

by

Kuei-Lin Chang

Master of Science in Chemistry

University of California, San Diego, 2015

Professor Charles L. Perrin, Chair

The kinetics of chalcone formation via aldol condensation was studied using UV spectrophotometry. Chalcone was formed from substituted benzaldehyde (ArCHO) and acetophenone (Ar'$COCH_3$) with catalyst sodium hydroxide (NaOH) dissolved in acetonitrile and H_2O or deuterium oxide (D_2O). The rate of appearance of each chalcone was measured at its λ_{max} using a UV spectrophotometer, and time curves of Absorbance vs. Time were analyzed. The rate expression for the formation of chalcone is third order: Rate = k_3 [ArCHO][Ar'$COCH_3$][$^-$OH]. With excess [Ar'$COCH_3$], the reaction becomes

pseudo first order in [ArCHO], where the observed rate constant (k_{obs}) is simply proportional to the concentrations of [Ar'COCH$_3$] and [$^-$OH]. Kinetic runs with different initial conditions of [ArCHO], [Ar'COCH$_3$], and [$^-$OH] were prepared in H_2O and in D_2O to measure the rates and the kinetic isotope effect k_D/k_H. The formation of chalcone or substituted chalcone was observed to be faster in D_2O than in H_2O, which indicates that Deprotonation 2 is not the rate-limiting step. Using a process of elimination, we can conclude that the rate-limiting step for chalcone mechanism via aldol condensation is the Elimination step in the dehydration process. The intermediate β-hydroxy ketone in each chalcone formation was synthesized. The β-hydroxy ketone intermediates were reacted with NaOH to revert to starting materials ArCHO and Ar'COCH$_3$, and to dehydrate to product chalcone. The ratio of concentration of starting material to product was determined and the rate constants from each β-hydroxy ketone intermediate to its starting materials and product were evaluated to help complete the understanding of the mechanism of chalcone formation.

I. INTRODUCTION

The importance of chalcone and its mechanism

Benzalacetophenone, the α, β unsaturated ketone also known as Chalcone, can be used to synthesize many useful derivatives. Chalcone and derivatives have application in a variety of areas including artificial sweeteners [1-4], scintillator [5], polymerization catalysis [6,7], and fluorescent whitening agents [8]. Chalcone can be prepared from benzaldehyde and acetophenone with catalyst sodium hydroxide via aldol condensation. We are interested in this base-catalyzed reaction because the reaction of chalcone formation has been used as a model reaction of aldol condensation in textbook for many years. However, the complete mechanism of chalcone formation has not yet been fully understood. The most essential piece in the mechanism of a reaction, the rate-limiting step, is still a puzzle for the chalcone formation. The rate-limiting step is important because it is the slowest step of the reaction that the whole rate of reaction mainly depends on. We are trying to study the kinetics and isotope effect of the chalcone formation via aldol condensation using UV spectrophotometry to help us determine the rate-limiting step of the reaction.

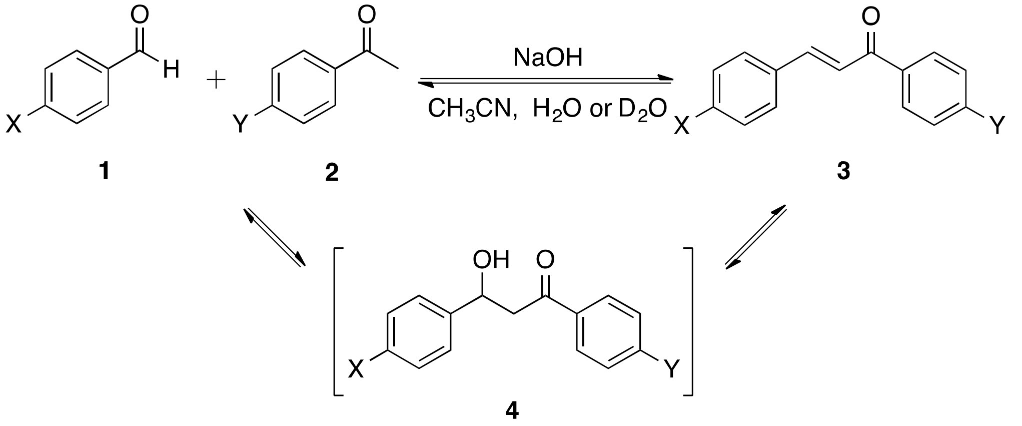

Scheme 1. Chalcone **3** formed from substituted aldehyde **1** and acetophenone **2** through the intermediate of the reaction β-hydroxy ketone **4** via aldol condensation.

Substituted **1** and **2** were used to synthesize **3a-f** and their intermediates **4a-f**. In Table 1, several functional groups such as chloro, nitro, and methyl were used to replace H at the para position of **1** and **2** to synthesize different **3** and **4**. The effect from electron withdrawing and donating groups to the reaction was compared and studied. All the names and chemical structures of **3a-f** and **4a-f** are reported in Table 2.

Table 1. Substituents of aldehyde **1a-d** and acetophenone **2a-c** reacted to produce chalcone products **3a-f** through their corresponding intermediate **4a-f**.

Entry	X (1)	Y (2)	Intermediate (4)	Product (3)
1	H (**1a**)	H (**2a**)	**4a**	**3a**
2	Cl (**1b**)	H (**2a**)	**4b**	**3b**
3	NO_2 (**1c**)	H (**2a**)	**4c**	**3c**
4	CH_3 (**1d**)	H (**2a**)	**4d**	**3d**
5	H (**1a**)	Cl (**2b**)	**4e**	**3e**
6	H (**1a**)	NO_2 (**2c**)	**4f**	**3f**

Table 2. Name and structure of each chalcone **3a-f** and its intermediate **4a-f**.

Entry	Product (3)	Intermediate (4)
1	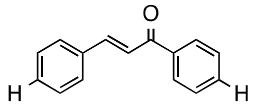 1,3-Diphenyl-2-propen-1-one **(3a)**	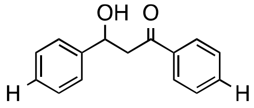 3-Hydroxy-1,3-diphenylpropane-1-one **(4a)**
2	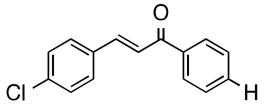 3-(4-Chlorophenyl)-1-phenyl-2-propen-1-one **(3b)**	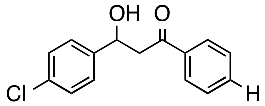 3-Hydroxy-3-(4-chlorophenyl)-1-phenylpropan-1-one **(4b)**
3	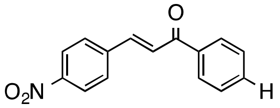 3-(4-Nitrophenyl)-1-phenyl-2-propen-1-one **(3c)**	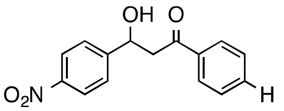 3-Hydroxy-3-(4-nitrophenyl)-1-phenylpropan-1-one **(4c)**
4	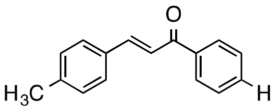 3-(4-Methylphenyl)-1-phenyl-2-propen-1-one **(3d)**	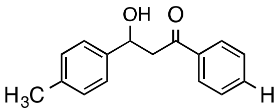 3-Hydroxy-3-(4-methylphenyl)-1-phenylpropan-1-one **(4d)**
5	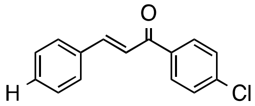 1-(4-Chlorophenyl)-3-phenyl -2-propen-1-one **(3e)**	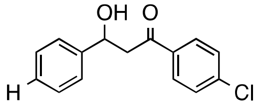 3-Hydroxy-1-(4-chlorophenyl)-3-phenylpropan-1-one **(4e)**
6	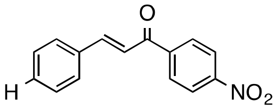 1-(4-Nitroophenyl)-3-phenyl -2-propen-1-one **(3f)**	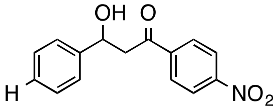 3-Hydroxy-1-(4-nitrophenyl)-3-phenylpropan-1-one **(4f)**

Mechanism and rate expression of chalcone formation

The mechanism of chalcone formation via aldol condensation has four main steps that are Deprotonation 1, Addition, Proton Equilibration, and Dehydration, where dehydration process can be divided into two separate steps, Deprotonation 2 and Elimination.

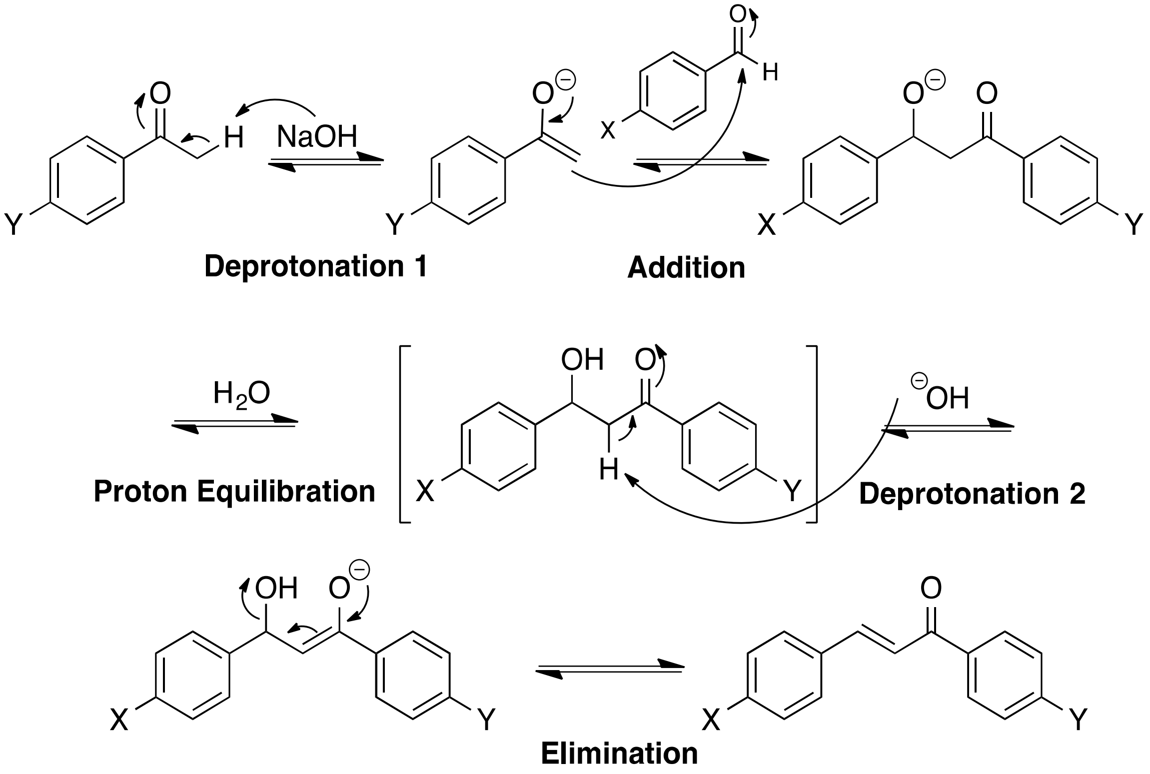

Scheme 2. Mechanism of chalcone formation via aldol condensation.

The rate expression for each step is combined in order to obtain the final rate expression for the mechanism. The intermediate β-hydroxy ketone **4** and its conjugate base are expressed as I and I^-, and the enolate [ArCH(OH)–CH=C(–O^-)Ar'] is expressed as I'^{-}. After substituting, the final rate expression of chalcone formation is determined to be third order: Rate = k_3[ArCHO][Ar'COCH$_3$][$^{-}$OH]. [9]

Rate = $d[Ar'COCH_2^{-}]/dt = k_1\,[Ar'COCH_3][\,^{-}OH]$ Deprotonation 1

Rate = $d[I^{-}]/dt = k_2\,[Ar'COCH_2^{-}][ArCHO]$ Addition

Rate = $d[I]/dt = k_3\,[I^{-}]$ Proton Equilibration

Rate = $d[I'^{-}]/dt = k_4\,[I][\,^{-}OH]$ Deprotonation 2

Rate = $d[ArCH{=}CHC({=}O)Ar']/dt = k_5\,[I'^{-}]$ Elimination

The third order rate expression is more complicated to observe and analyze, so excess **2** can be used to reach pseudo first order. The large concentration of **2** will become constant. As the catalyst of the reaction, sodium hydroxide can be considered as constant as well, and the rate of chalcone formation will depend only on concentration of **1** with the rate constant observed (k_{obs}) equals to third order forward rate constant (k_3) times the concentration of **2** and sodium hydroxide.

$$\text{Rate} = k_{obs}[ArCHO]$$

$$k_{obs} = k_3[Ar'COCH_3][\,^{-}OH]$$

The Deprotonation 1 cannot be the rate-limiting step because the reaction is first order in [ArCHO], [Ar'COCH$_3$], and [$^{-}$OH]. During Deprotonation 1, [ArCHO] is not present in the transition state, hence, this step cannot be rate-limiting. The rate-limiting step is the slowest step of a reaction that determines the rate of the overall chemical reaction. Therefore, Proton Equilibration is very unlikely to be the rate-limiting step as "proton transfer reactions between oxygen atoms are usually very fast".[10] We have now left with Addition and Dehydration steps. According to Noyce, Pryor, and Bottini's observation, "alkali transforms the intermediate β-hydroxy ketone to benzaldehyde and acetophenone more rapidly than it dehydrates." Their experiment suggested that the Addition step is faster than the Dehydration step, indicating that Addition step cannot be rate-limiting.[11] Since Deprotonation 1, Addition, and Proton Equilibration steps are eliminated, the rate-limiting step must be either Deprotonation 2 or Elimination step in the final Dehydration process,

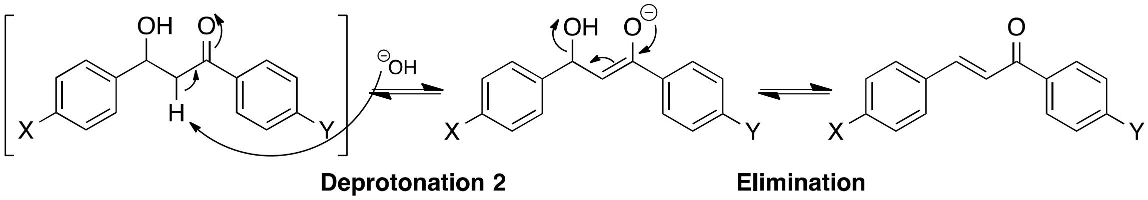

(Dehydration Process)

We are trying to determine whether the rate-limiting step of the mechanism of chalcone formation via aldol condensation is the removal of proton to form enolate Deprotonation 2 or the leaving of hydroxide group and forming a double bond Elimination in the dehydration process. In order to approach the goal, the kinetics and isotope effect of chalcone formation via aldol condensation are studied using UV spectrophotometry. Our ultimate goal is to find out the rate-limiting step of formation of several substituted chalcones using isotope effect for each chalcone by comparing rate of reaction in H_2O and D_2O, and to have complete understanding of the energy diagram of the reaction by determining the separate rate constants of each chalcone's intermediate converting to its starting materials and product.

Isotope effect study

Deuterium (D or ^{2}H) is the isotope of hydrogen that contains 1 proton and 1 neutron while hydrogen (^{1}H) only has a single proton. Deuterium oxide (D_2O), also known as heavy water, is often used for isotope effect study. When H and D are exchanged, the compound will have different reactivity because of their difference in vibrational frequency (ν)□ [12] As Hooke's Law states, $\nu = \frac{1}{2\pi}\sqrt{\frac{k}{\mu}}$ where $\mu = \frac{m_1 m_2}{m_1 + m_2}$, the difference in mass of H and D causes the change of vibrational frequency. The rate-limiting step of chalcone formation via aldol condensation can be studied by observing the kinetic isotope effect of the reaction using H_2O and D_2O as solvent. The breaking of a C-H bond in H_2O and a C-D bond in D_2O in Deprotonation 2 step of chalcone formation can be compared and studied using isotope effect because of the difference of their bond strength due to vibrational frequency.

II. EXPERIMENTAL METHODS

Instrumentation

All UV kinetic data and spectra were obtained using UV spectrophotometer (UV-1800), Shimadzu Corporation, SN. A11454500450 CD. Solution for kinetic experiments was transferred into quartz cuvettes for measuring ultraviolet region by UV spectrophotometry. Absorbance smaller than 2.0 was considered more reliable, so 1 mm, 2 mm, and 10 mm quartz cuvettes were used depending on concentration of solution. All NMR spectra were obtained on JEOL ECA500 FT-NMR spectrometer (500.2 MHz ^{1}H) using chloroform ($CDCl_3$) as solvent to make sure all **4** were successfully synthesized. Melting points range of all **3** and **4** were measured using Mel-Temp to check purity and compare with literature.

Synthesis of chalcone

Chalcone product **3** was synthesized following the procedure described in Noyce's paper. A solution of 0.005 mole of **1,** 0.005 mole of **2**, and 0.015 mole sulfuric acid in 10 ml of acetic acid was stirred for 48 hours at room temperature to produce **3**. [13] When the reaction was completed, the solution was diluted with water and filtered to collect **3** crystals. Recrystallizations were done in suitable solvents including dichloromethane (DCM) mixed with hexane or toluene to afford pure crystals, as listed in Table 3 Purity was then checked by melting points and NMR spectra.

Table 3. Crystallization solvent, observed melting points, and literature melting points for chalcone **3a**-**f**.

	Crystallization Solvent	m.p.	Literature m.p.
3a	DCM & Hexane	52.8-56.7°C	lit. [14] 55-57°C
3b	DCM & Hexane	108.6-115.0°C	lit. [13] 113-114°C
3c	Toluene	160.2-164.8°C	lit. [13] 163°C
3d	DCM & Hexane	91.7-93.1°C	lit. [14] 93.2°C
3e	DCM & Hexane	87.3-91.0°C	lit. [15] 90-92°C
3f	DCM & Hexane	145.3-148.5°C	lit. [16] 146.5-147°C°C

Finding λ_{max} for specific chalcone product

Before measuring the rate of appearance of **3** by UV spectrophotometry to obtain the observed rate constants (k_{obs}), the λ_{max} of each **3** must be found. Chalcone product was synthesized and diluted with acetonitrile and H_2O into a suitable concentration for UV spectrophotometry to read spectrum and find the λ_{max} and the extinction coefficient. Figure 1 shows the spectrum of a representative chalcone.

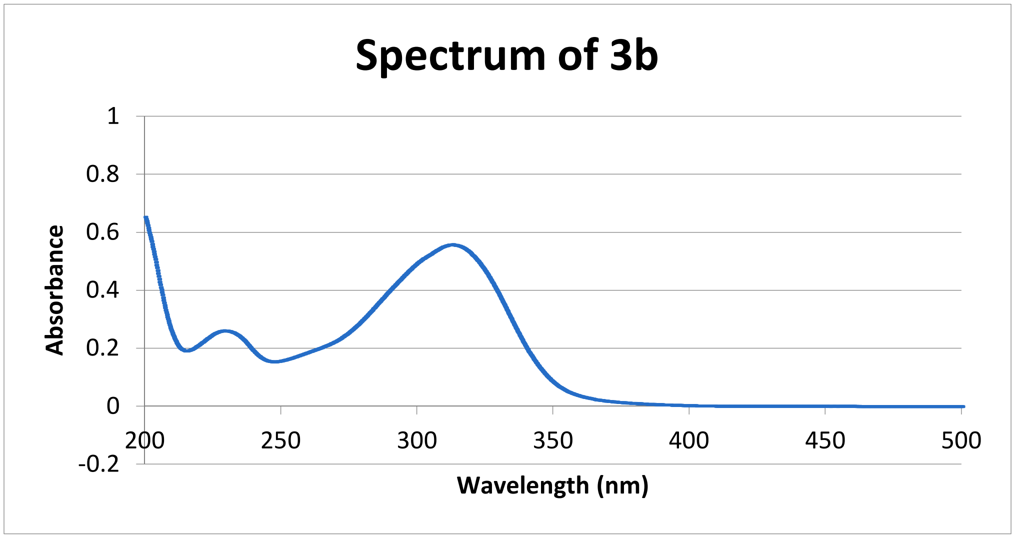

Figure 1. Spectrum of **3b** measured by UV spectrophotometer to find the λ_{max} at around 312nm.

Preparation of solutions for kinetic measurements

Vacuum distillation was used to purify **1a** and **2a** under vacuum pressure 10 torr at vapor pressure 75.0°C and 82.0°C respectively. Nitrogen gas was pumped into solution for storing purpose before use. All purified organic liquids and crystals **1**, **2**, **3**, and **4** were dissolved in acetonitrile and diluted in volumetric flasks with H_2O or D_2O to the concentrations needed. NaOH and NaCl solutions were dissolved in H_2O or D_2O. Cuvettes and volumetric flasks were oven dried before running kinetic experiment to make sure that there was no additional H_2O in reaction. When measuring observed rate constants (k_{obs}) by UV spectrophotometry, excess **2** was mixed with **1** and catalyst NaOH in a total of 10 ml solution in volumetric flask to reach pseudo first order reaction conditions. In each kinetic run, the salt concentration and amount of acetonitrile in 10 ml solution were kept the same to insure that the reaction reacted under the same solvent condition. Various initial conditions for the concentrations of **1**, **2**, and NaOH were used for kinetic runs to measure the observed rate constant (k_{obs}) for the pseudo first order reaction.

Kinetic experiments to determine isotope effect

When mixing the reagents, **1** was added last to the solution, and the reaction started to proceed to **3**. The solution was then quickly transferred from volumetric flask into cuvette to measure the rate of formation of **3**, and the absorbance at the λ_{max} of **3** was taken every 30 seconds using UV spectrophotometer until the reaction neared completion. Time curves of absorbance vs. time in minutes were generated to see whether reaction successfully approached completion. The kinetic experiments were run in H_2O and in D_2O to compare the third order forward rate constants of the reaction and calculate isotope effect k_D/k_H for each **3**.

Calculation of observed rate constants (k_{obs})

The kinetic data of absorbance vs. time was analyzed in Excel by nonlinear least squares to calculate the observed rate constants (k_{obs}). Equation 1 was used to calculate absorbance to compare with the observed. As initial estimates, we used the first absorbance for initial absorbance (A_0), last absorbance for infinity absorbance (A_∞), and an approximate guess for observed rate constant (k_{obs}) to calculate each absorbance (A) at its specific time (t). Deviations between actual and theoretical absorbance were calculated by squaring their differences. Equation 2, which is the minimum value of the sum of squares of all deviations, was then found by adjusting three variable cells A_0, A_∞, and k_{obs} using program in Excel called “Solver”. The best-fit observed rate constants (k_{obs}) were generated.

$$A = A_\infty - (A_\infty - A_0)\, e^{-k_{obs}t} \qquad \text{Equation 1}$$

$$\sum [A_{obs} - (A_\infty - (A_\infty - A_0)e^{-k_{obs}t}]^2 \qquad \text{Equation 2}$$

Calculation of third order forward rate constants (k_3)

When the observed rate constants (k_{obs}) for each set of kinetic experiment were found, we used two methods to obtain k_3, the third order forward rate constant of chalcone formation. One way is to plot k_{obs}/[NaOH] against [Ar'$COCH_3$] as suggested by Guthrie. The slope of the line, evaluated by linear least squares, is equal to the third order forward rate constant (k_3), and the intercept represents the reverse rate constant (k_r). [17]

We can also use the equilibrium law to calculate k_3 in H_2O and D_2O for each **3**. Since we know that the k_{obs} measured using UV spectrophotometer is the sum of the forward rate constant (k_f) and reverse rate constant (k_r) of the reaction, we can use Equation 3 and 4 to get k_f, the forward rate constants of the reaction that we are interested in. K_e for each kinetic experiment can be calculated using Equation 5 since we know the concentration of **1**, **2** and **3**. After substituting Equations 3-5, Equation 6 can be used to calculate the forward rate constant of the reaction (k_f). K_e calculated from each kinetic run should be somewhat similar to each other for each formation of **3** in the same solvent .The light weighted error propagation ($\sqrt{w}$) in Equation 7 is used to correct errors of some extreme K_e calculated from each kinetic run. Equation 8 can be used to obtain the corrected K_e using error propagation. The average of corrected K_e in H_2O and D_2O of formation of each **3** are listed in Table 4.

The purpose of the project was to compare the forward rate constants of formation of **3** in H_2O and D_2O to determine which step of reaction is rate-limiting, so reverse rate constants (k_r) for formation of chalcone are not reported.

$$\mathrm{k_{obs}} = \mathrm{k_f[Ar'COCH_3][^{-}OH] + k_r[^{-}OH]} \qquad \text{Equation 3}$$

$$\mathrm{K_e} = \frac{\mathrm{k_f}}{\mathrm{k_r}} \qquad \text{Equation 4}$$

$$\mathrm{K_e} = \frac{[\mathbf{3}]_\infty}{[\mathbf{1}]_\infty[\mathbf{2}]} = \frac{[\mathbf{3}]_\infty}{([\mathbf{1}]_0 - [\mathbf{3}]_\infty)[\mathbf{2}]} \qquad \text{Equation 5}$$

$$\mathrm{k_f} = \frac{\mathrm{k_{obs}}}{(\frac{1}{\mathrm{K_e}} + 1)} \times \frac{1}{\mathrm{[Ar'COCH_3][\ ^{-}OH]}} \qquad \text{Equation 6}$$

$$\sqrt{\mathrm{w}} = \sqrt{\frac{1}{\mathrm{K_e}^2\,[\frac{1}{[\mathbf{3}]_\infty{}^2} + \frac{1}{([\mathbf{1}]_0 - [\mathbf{3}]_\infty)^2}]}} \qquad \text{Equation 7}$$

$$\text{Weighted } \mathrm{K_e} = \frac{\sum(\sqrt{\mathrm{w}} \times \mathrm{K_e})}{\sum\sqrt{\mathrm{w}}} \qquad \text{Equation 8}$$

Table 4. Average K_e and corrected K_e of formation of each **3**.

Chalcone	**K_e (M^{-1})**	**Weighted K_e (M^{-1})**
3a	5.55	4.63
3b	147	15.2
3c	354	204
3e	120	97.1
3f	83.8	79.5

Synthesis of ketol intermediate

β-hydroxy ketone intermediate **4** was synthesized via MgI_2-promoted aldol reaction from **1** and **2** in Scheme 3 following procedures described in Wei's paper, [18] but with 5 times larger scale. A 100 ml round bottom flask was loaded with 25 ml distilled dichloromethane, MgI_2 (1.7 g, 6.0 mmol) , **1** (1.0 equiv), and **2 (**1.2 equiv). Diisopropylethylamine iPr_2EtN (1.15 ml, 6.5 mmol) was added dropwise to the solution, and the reaction mixture was stirred for at least 30 min at room temperature before quenching it with 20 ml of 2N HCl. [18] Solution was extracted with CH_2Cl_2 and washed with H_2O. The organic layer was dried with $MgSO_4$ and concentrated with rotovap. The dark brown crude product was purified by flash chromatography with increasing polarity of solvent system (hexane/ethyl acetate) to separate intermediate **4** from starting materials **1** and **2**. Collected fractions were spotted on TLC plate, developed in a jar with solvent system (hexane/ethyl acetate 6:1), and visualized under UV light. Fractions containing **4** were combined and evaporated. After crystallizing from the indicated solvent mixture in Table 5, clear crystals were obtained. Purity was checked through melting points and NMR spectra.

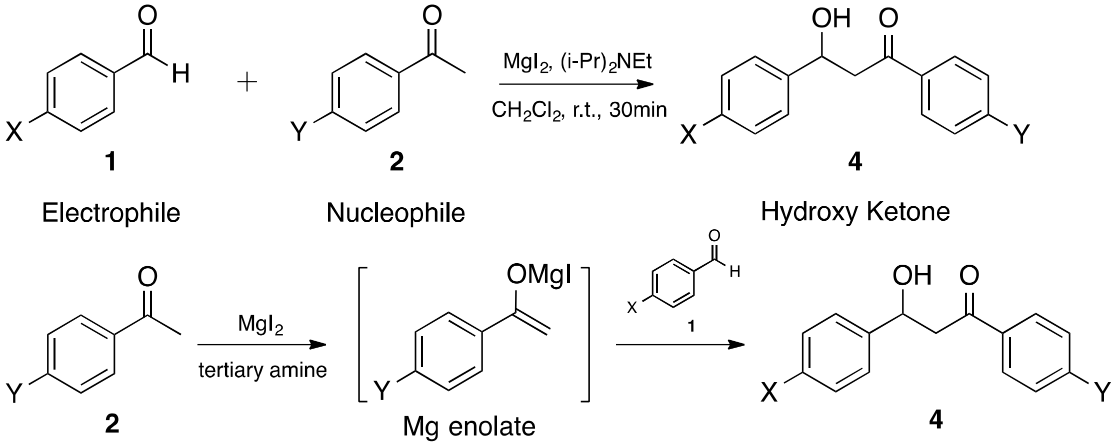

Scheme 3. Synthesis of β-hydroxy ketone intermediate **4** via MgI_2-promoted aldol reaction from **1** (Electrophile) and **2** (Nucleophile). [18]

Table 5. Crystallization solvent, observed melting points, and literature melting points for intermediate **4a**-**f**.

	Crystallization Solvent	**m.p.**	**Literature m.p.**
4a	DCM & Hexane	47.2-48.1°C	lit. [19] 53-54°C
4b	DCM & Hexane	93.6-95.2C	lit. [20] 96-96.5°C
4c	DCM & Hexane	111.3-112.7°C	lit. [21] 112.9 °C
4d	DCM & Hexane	49.1-51.6°C	lit. [22] 47-48°C
4e	DCM & Hexane	52.5-56.7°C	N/A
4f	DCM & Hexane	86.5-87.4°C	lit. [23] 90°C

3-Hydroxy-1,3-diphenylpropane-1-one (4a)
Crystallization solvent: DCM & Hexane
Yellow solid; mp: 47.2-48.1°C (lit.[19] 53-54°C).
^{1}H NMR (500 MHz, $CDCl_3$): δ = 3.38 (d, 2H), 3.58 (br s, 1H), 5.35 (m, 1H), 7.32 (m, 1H), 7.39 (m, 2H), 7.46 (m, 4H), 7.59 (m, 1H), 7.96 (m, 2H); ^{1}H NMR lit.[18]

3-Hydroxy-3-(4-chlorophenyl)-1-phenylpropan-1-one (4b)
Crystallization solvent: DCM & Hexane
White solid; mp: 93.6-95.2C (lit.[20]96-96.5°C).
^{1}H NMR (500 MHz, $CDCl_3$): δ = 3.34 (m, 2H), 3.64 (br s, 1H), 5.32 (m, 1H), 7.37 (m, 4H), 7.48 (m, 3H), 7.60(m, 1H), 7.95 (m, 2H) lit.[24].

3-Hydroxy-3-(4-nitrophenyl)-1-phenylpropan-1-one (4c)
Crystallization solvent: DCM & Hexane
White solid; mp: 111.3-112.7°C (lit.[21] 112.9 °C).
^{1}H NMR (500 MHz, $CDCl_3$): δ = δ = 3.37 (m, 2H), 3.82 (br s, 1H), 5.46 (m, 1H), 7.49 (m, 2H), 7.61 (m, 3H), 7.94 (m, 2H), 8.24 (m, 2H) lit.[21]

3-Hydroxy-3-(4-methylphenyl)-1-phenylpropan-1-one (4d)
Crystallization solvent: DCM & Hexane
White solid; mp: 49.1-51.6°C (lit.[22] 47-48°C).
^{1}H NMR (500 MHz, $CDCl_3$): δ = 2.35 (s, 3H), 3.37 (m, 2H), 3.51 (br s, 1H), 5.32 (t, 1H), 7.19 (d, 2H), 7.33 (d, 2H), 7.47 (m, 2H), 7.59 (m, 1H), 7.95 (m, 2H) lit.[24]

3-Hydroxy-1-(4-chlorophenyl)-3-phenylpropan-1-one (4e)
Crystallization solvent: DCM & Hexane
White solid; mp: 52.5-56.7°C (lit°C).
^{1}H NMR (500 MHz, $CDCl_3$): δ = 3.37 (m, 3H), 5.34 (m, 1H), 7.25-7.45 (m, 7H), 7.90 (m, 2H) lit.[24]

3-Hydroxy-1-(4-nitrophenyl)-3-phenylpropan-1-one (4f)
Crystallization solvent: DCM & Hexane
Yellow solid; mp: °C (lit.[23] 90°C).
^{1}H NMR (500 MHz, $CDCl_3$): δ = 3.14 (br s, 1H), 3.41 (m, 2H), 5.38 (m, 1H), 7.23-7.63 (m, 5H), 8.11(m, 2H), 8.29 (m, 2H) lit.[23].

Isosbestic point of 1 and 2

The extinction coefficients of starting materials **1** and **2** and chalcone **3** are essential for determining the ratio of starting material to product formed from each intermediate ketol **4**. Because the maximum absorbances of **1** and **2** occurred at two different wavelengths, it was difficult to calculate the concentration of either starting material. Since we know **1** and **2** have the same concentration due to stoichiometry, we can simulate spectra of **1** and **2** with the same concentration. Isosbestic point was found when the simulated spectra of **1** and **2** cross each other at the specific wavelength that their extinction coefficient are equal (Figure 2).

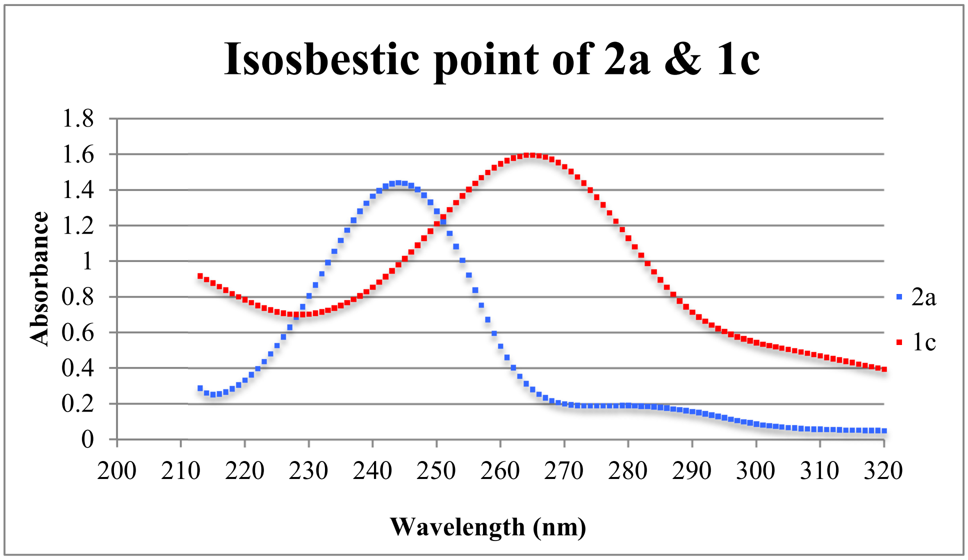

Figure 2. Isosbestic point of **2a** and **1c** at 251 nm found for calculating concentration of starting materials formed from **4c**.

Partitioning of intermediate to starting materials and to product

Each synthesized intermediate **4** was dissolved in acetonitrile and diluted with H_2O to the suitable concentration for UV spectrophotometry. **4** was mixed with 0.2M NaOH in a total of 10 ml solution with enough acetonitrile to keep everything dissolved. The reaction should be completed immediately with the high concentration of NaOH used. When NaOH was added, a fraction of **4** reverted back to starting materials **1** and **2,** and the remainder dehydrated to the product **3** at the same time. The solution was transferred into cuvette and the spectrum was taken. The isosbestic point for **1** and **2** was found prior to the study of **4** reacting with base. Since **1** and **2** have the same extinction coefficient at isosbestic point, we can double it to have a combined extinction coefficient for **1** and **2** ideally to help us calculate the concentration of either starting materials formed from **4** in Equation 9 using Beer's law. However, chalcone **3** contributed some absorbance at the isosbestic point of **1** and **2**, and starting materials **1** and **2** did as well at **3**'s λ_{max}. So Equation 10 was used to solve for concentration of [**1**] or [**2**] and chalcone [**3**] using the absorbance at isosbestic point of **1** and **2** and λ_{max} of **3** formed from **4** reacting with base. The ratio of concentration of either **1** or **2** to chalcone **3** was determined using Equation 11 to show how much faster was the rate from intermediate to starting materials than to product.

$$A(\lambda\,\text{isosb}) = (\varepsilon_1[\mathbf{1}] + \varepsilon_2[\mathbf{2}])l, \qquad \varepsilon_1 = \varepsilon_2 \; and \; [\mathbf{1}] = [\mathbf{2}]$$

$$[\mathbf{1}] = [\mathbf{2}] = \frac{A(\lambda\,\text{isosb})}{2\varepsilon l}$$

Equation 9

$$A(\lambda\,\mathbf{3}) = (\varepsilon_{3\,at\,\lambda\,\mathbf{3}}[\mathbf{3}] + \varepsilon_{1\,at\,\lambda\,\mathbf{3}}[\mathbf{1}] + \varepsilon_{2\,at\,\lambda\,\mathbf{3}}[\mathbf{2}])l$$

$$A(\lambda\,\text{isosb}) = (\varepsilon_{3\,at\,\lambda\,\boldsymbol{isosb}}[\mathbf{3}] + 2\varepsilon_{\text{at}\,\lambda\,\boldsymbol{isosb}}[\mathbf{1}])l$$

Eqaution10

$$R = \frac{[\mathbf{1}] \; or \; [\mathbf{2}]}{[\mathbf{3}]}$$

Equation 11

Calculation of rate constants from intermediate to starting materials and to product

After knowing (R), the ratio of concentration of either **1** or **2** to chalcone **3** formed from **4** to both directions, kinetic experiment was run to measure the observed rate constant from **4** to **1**, **2**, and **3** combined in Equation 12. Since the half lives for rate of disappearance of **4** and rate of appearance of **3** are the same, we can measure k_{obs} by following the rate of appearance at **3**'s λ_{max}. An example of time curve is shown in Figure 3 for each **4** reacting with low NaOH concentration was measured at each **3**'s λ_{max}. The measured k_{obs} is equal to k_2 times concentration of NaOH ($k_{obs} = k_2[^{-}OH]$), where k_2 is the total rate constant for the disappearance of **4**. Less concentrated NaOH was mixed with **4** to slow down the reaction for UV spectrophotometer to observe the change of concentration over time. Kinetic data was analyzed using Solver in Excel to calculate the k_{obs}, which was then divided by the NaOH concentration used to obtain the total rate constants for both directions k_2. In Equation 13, the rate for disappearance of **4** is equal to the sum of the rate from **4** to **3** times the fraction of **4** that goes to chalcone (f_c) plus the rate from **4** to **1** and **2** times the fraction of **4** that goes to precursor (f_p). The ratio of concentration of starting material to product (R) in Equation 11 helps to find out the rate constants from **4** to **1** and **2** and to **3** using Equation 13-15.

$$-\frac{d}{dt}[\mathbf{4}] = k_2[^{-}OH][\mathbf{4}]$$

$$-\frac{d}{dt}[\mathbf{4}] = k_{obs}[\mathbf{4}] \qquad \text{Equation 12}$$

$$-\frac{d[\mathbf{4}]}{dt} = f_c\frac{d[\mathbf{3}]}{dt} + f_p\frac{d[\mathbf{1}\ or\ \mathbf{2}]}{dt} \qquad \text{Equation 13}$$

$$k\ (\mathbf{4}\ to\ \mathbf{3}): \frac{k_2}{R+1} \times\ 1 \qquad \text{Equation 14}$$

$$k\ (\mathbf{4}\ to\ \mathbf{1}\ and\ \mathbf{2}): \frac{k_2}{R+1} \times\ R+1 \qquad \text{Equation 15}$$

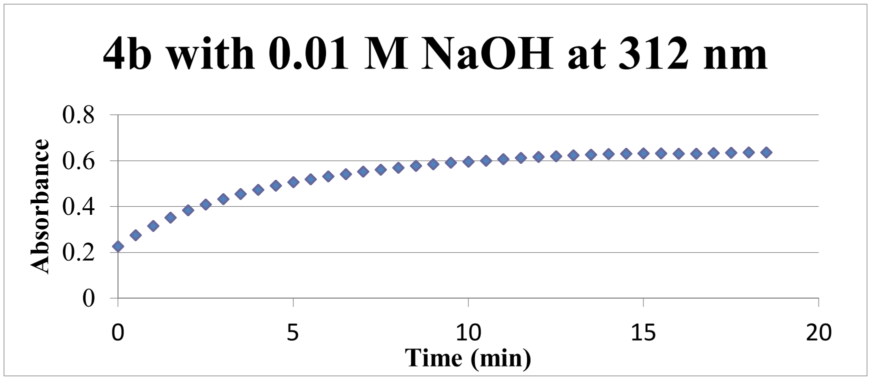

Figure 3. Time curve of 0.016M **4b** reacting with 0.01M NaOH to produce **3b** measured by UV spectrophotometer at 312 nm to obtain k_{obs}.

III. RESULTS

Kinetic time curve of chalcone formation

Figure 4 is an example of the Absorbance vs. Time curve for formation of chalcone **3a** under the initial condition of 0.00102M **1a**, 0.0216M **2a**, and 0.100M NaOH in D_2O was measured at 312nm, **3a**'s λ_{max}.

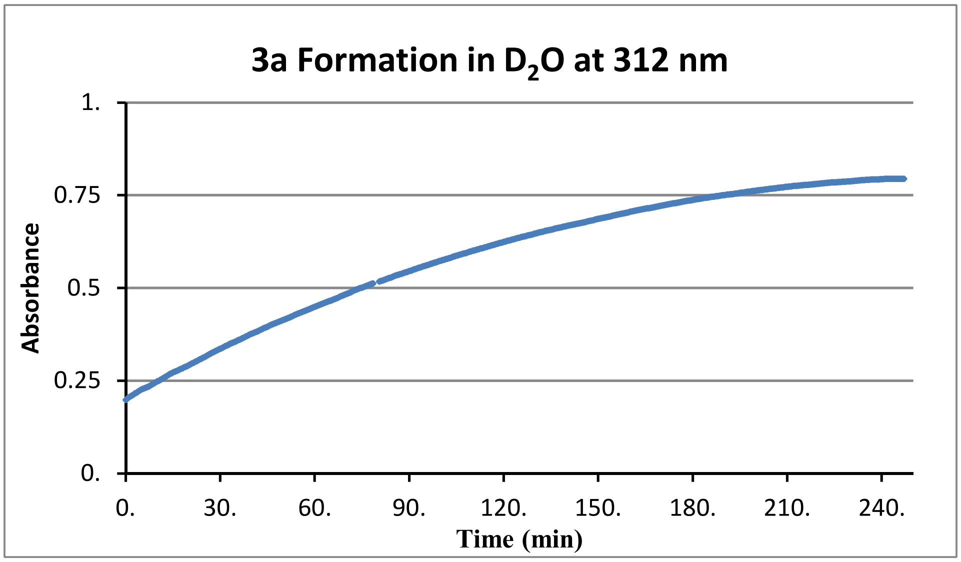

Figure 4. Absorbance vs. Time of **3a** formation in D_2O measured at 312 nm.

k_3 of chalcone formation in H_2O and D_2O via Guthrie's method

The third order forward rate constants in H_2O and D_2O for formation of **3a**, **3b**, and **3c**, **3e**, and **3f** were determined using Guthrie's method by plotting $k_{obs}/[OH^-]$, the observed rate constants (k_{obs}) for each kinetic run divided by NaOH concentration, against the concentration of **2**. The plot was expected to be linear, and the slope of the line is k_3, the third order forward rate constant of the formation of **3**. [17] The determined k_3 in H_2O and D_2O for formation of each **3** were shown in Figure 5– 9.

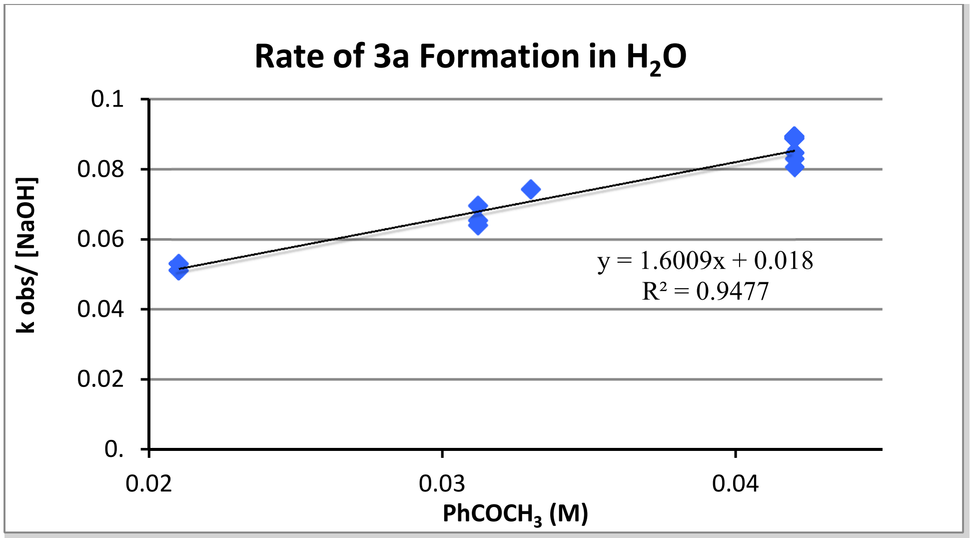

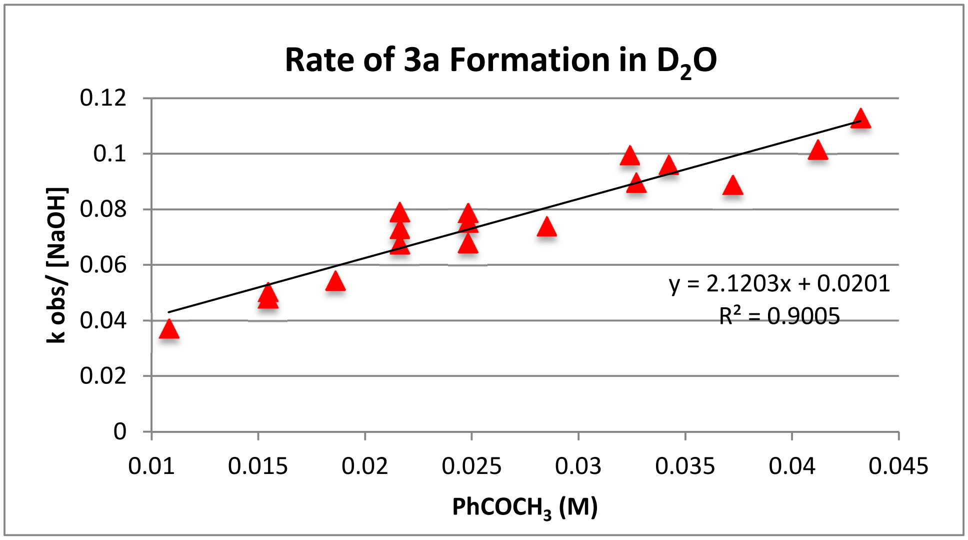

Figure 5. k_{obs}/ [NaOH] vs. [PhCOCH3] to obtain third order forward rate constants 1.60 $M^{-2}min^{-1}$ in H2O and 2.12 $M^{-2}min^{-1}$ in D2O for formation of **3a**.

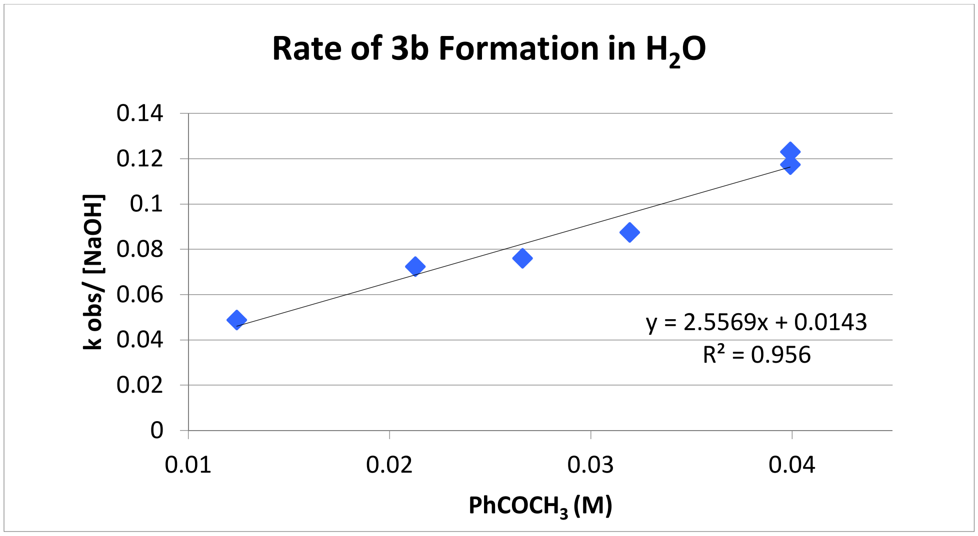

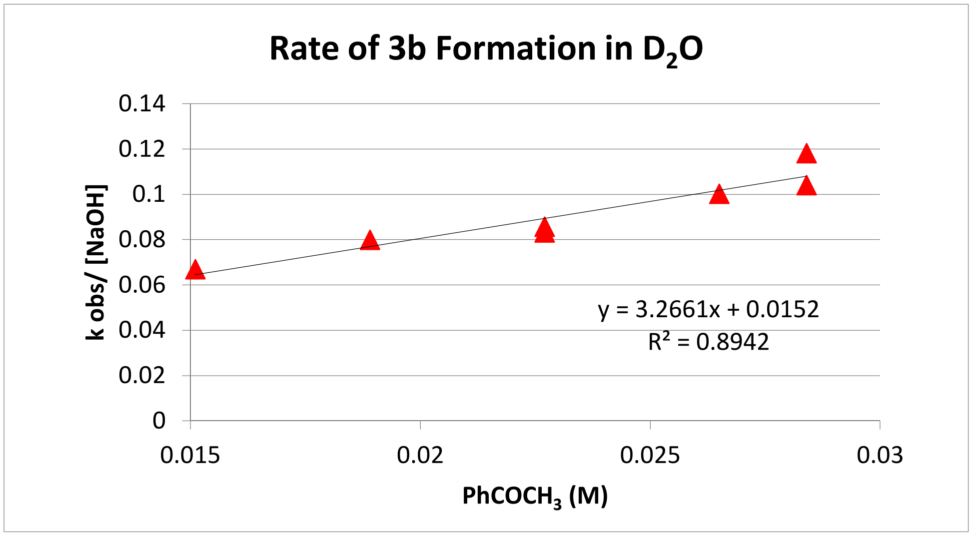

Figure 6. k_{obs}/ [NaOH] vs. [PhCOCH3] to obtain third order forward rate constants 2.56 $M^{-2}min^{-1}$ in H_2O and 3.27 $M^{-2}min^{-1}$ in D_2O for formation of **3b**.

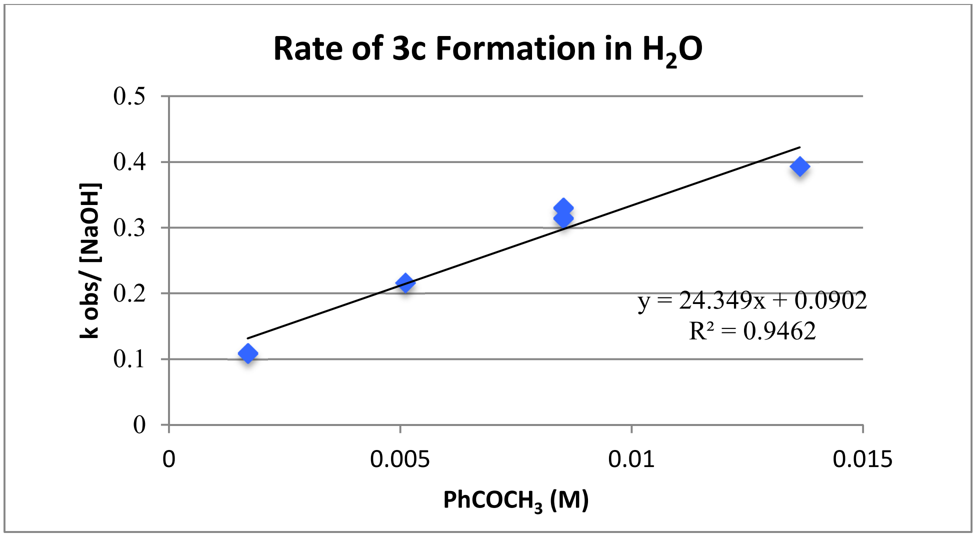

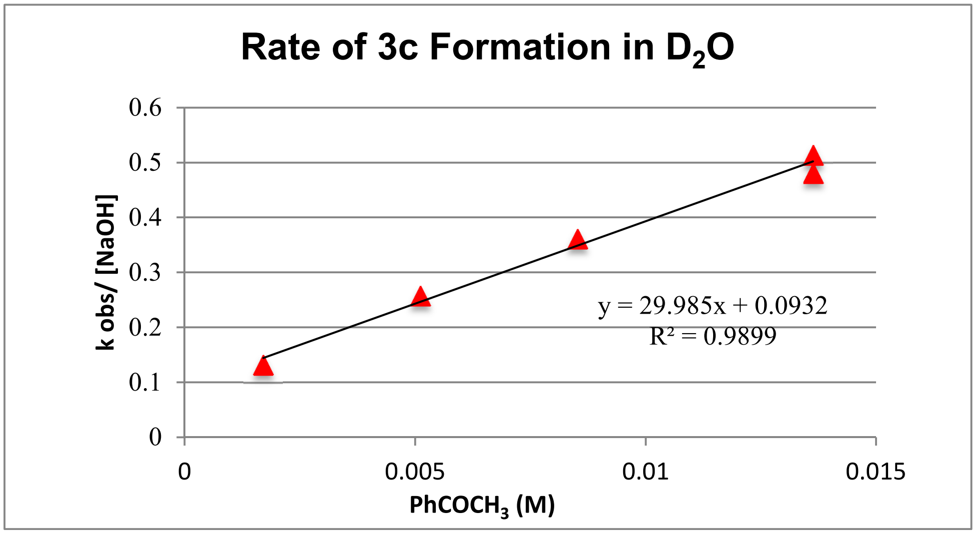

Figure 7. $k_{obs/}$ [NaOH] vs. [$PhCOCH_3$] to obtain third order forward rate constants 24.3 $M^{-2}min^{-1}$ in H_2O and 30.0 $M^{-2}min^{-1}$ in D_2O for formation of **3c**.

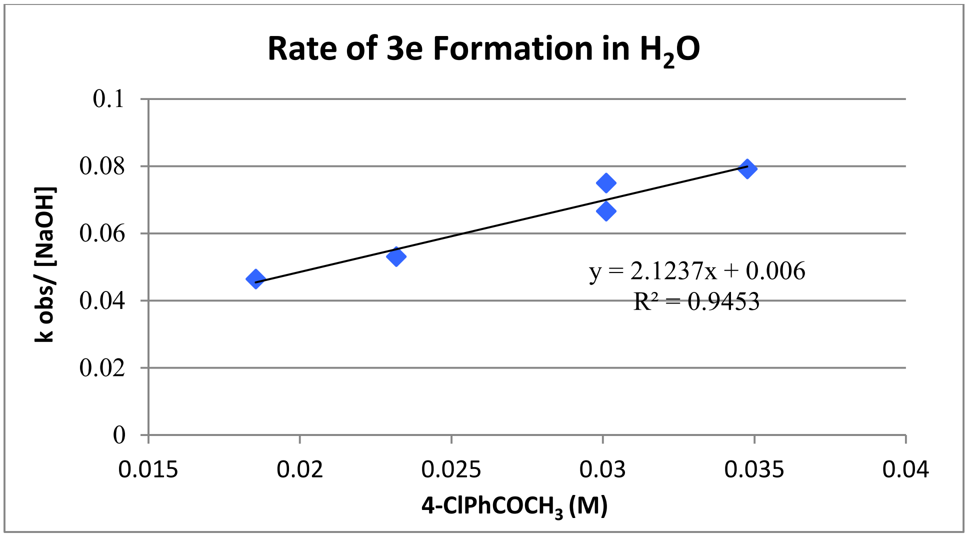

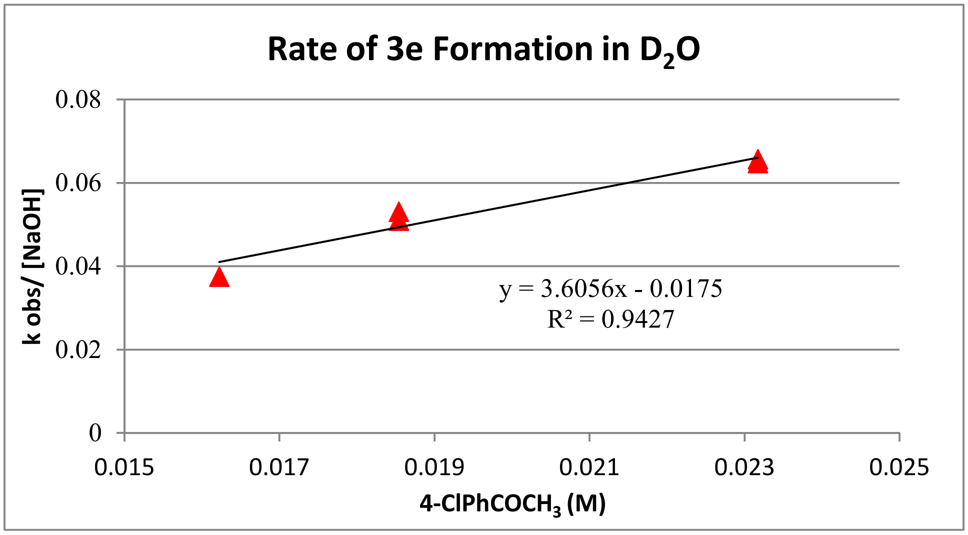

Figure 8. $k_{obs/}$ [NaOH] vs. [4-ClPhCOCH$_3$] to obtain third order forward rate constants 2.12 $M^{-2}min^{-1}$ in H_2O and 3.61 $M^{-2}min^{-1}$ in D_2O for formation of **3e**.

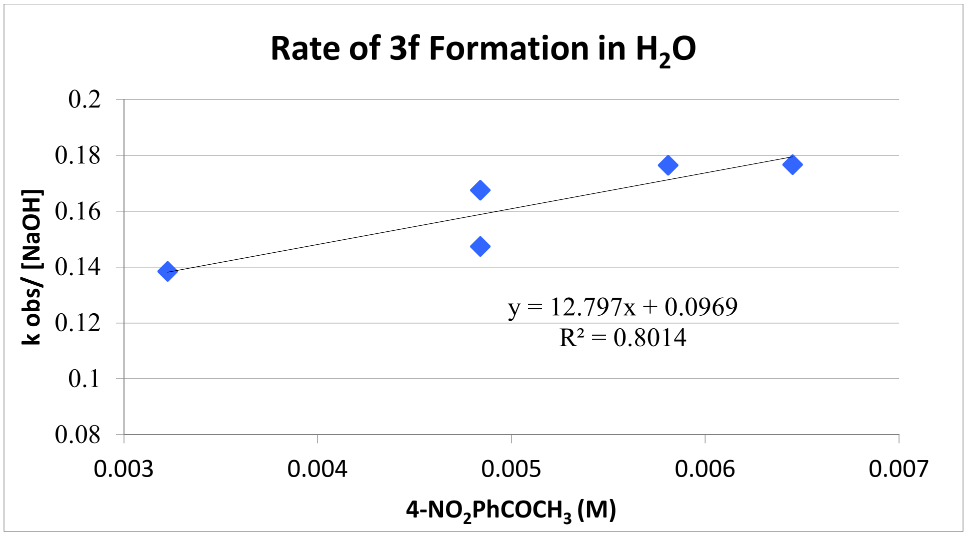

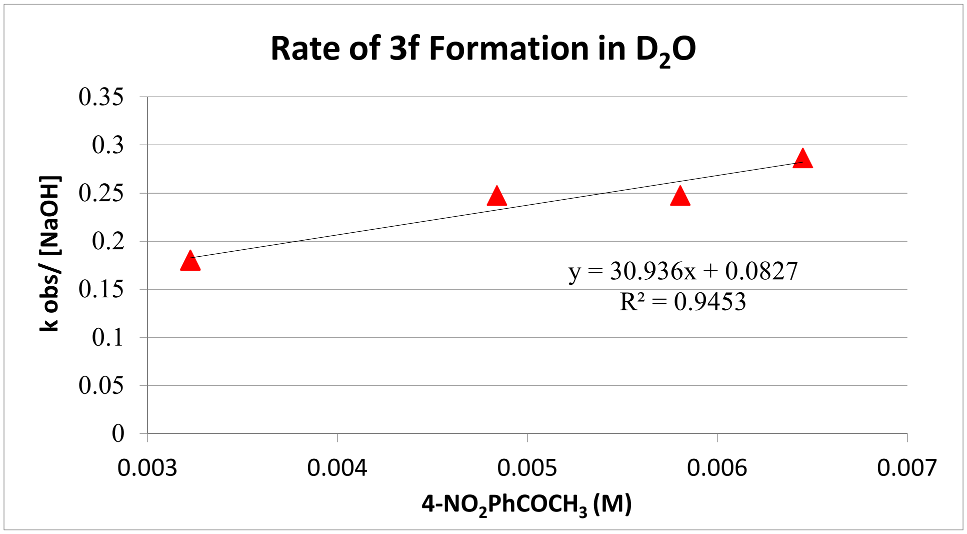

Figure 9. $k_{obs/}$ [NaOH] vs. [4-$NO_2PhCOCH_3$] to obtain third order forward rate constants 12.8 $M^{-2}min^{-1}$ in H_2O and 30.9 $M^{-2}min^{-1}$ in D_2O for formation of **3f**.

Isotope effect (k_D/k_H) of formation of 3

When k_3 in H_2O (k_H) and in D_2O (k_D) for formation of each **3** were found, the isotope effect k_D/k_H for formation of each **3** was determined. Normally, the isotope effect is reported as k_H/k_D. In this kinetic study for formation of **3**, however, k_3 in D_2O was faster than that in H_2O for formation of each **3**. Therefore, isotope effect was reported as k_D/k_H for formation of each **3** in along with the third order forward rate constants in H_2O (k_H) and in D_2O (k_D) obtained from Figure 5 - 9 via Guthrie's method. Another method is to use the equilibrium law to calculate k_3 of the reaction in H_2O and in D_2O. Table 7 includes the third order forward rate constants in H_2O (k_H) and in D_2O (k_D) and the isotope effect k_D/k_H calculated via Equations 3-8.

Table 6. k_3 in H_2O and D_2O calculated via Guthrie's method and isotope effect k_D/k_H for each **3**.

Chalcone	**Acetonitrile (%)**	**k_H ($M^{-2}min^{-1}$)**	**k_D ($M^{-2}min^{-1}$)**	**Isotope Effect (k_D/k_H)**
3a	26	1.60	2.12	1.33
3b	40	2.56	3.27	1.28
3c	40	24.3	30.0	1.23
3e	40	2.12	3.61	1.70
3f	40	12.8	30.9	2.41

Table 7. k_3 in H_2O and D_2O calculated via equilibrium law and isotope effect k_D/k_H for each **3**.

Chalcone	**Acetonitrile (%)**	**k_H ($M^{-2}min^{-1}$)**	**k_D ($M^{-2}min^{-1}$)**	**Isotope Effect (k_D/k_H)**
3a	26	1.78	2.45	1.38
3b	40	2.97	3.71	1.25
3c	40	42.0	48.3	1.15
3e	40	2.33	2.68	1.15
3f	40	32.8	49.4	1.51

Results for ketol intermediate analysis

According to Noyce's paper, when intermediate **4** reacts with NaOH, it proceeds to starting materials **1** and **2** and to product **3** simultaneously but with different rates.[11] All intermediate **4a-f** were synthesized and studied to determine the ratio of concentration of **1** or **2** to concentration of **3** formed from **4** when reacted with NaOH. When the isosbestic point of starting materials **1** and **2** was found, Equations 10 and 11 were used to calculate the concentrations of **1**, **2**, and **3** formed from **4** and the ratio (R), concentration of starting material over concentration of product, reported in Table 8. The average ratio (6:1) for each **4** in Table 8 shows that **1** and **2** formed from **4** is about 6 times faster than **3** formed from **4**, which is slightly different than the ratio (4:1)[11] reported by Noyce. The reason for that is because Noyce did not take the absorbance of starting materials at λ_{max} of **3** and the absorbance of **3** at λ_{max} of starting materials into account when evaluating the concentration and ratio. The rate constant (k_2) for disappearance of **4** was calculated from k_{obs} using Equation 12. Knowing k_2 and ratio (R) for each **4**, the rate constants from **4** to **1** and **2** and to **3** were determined using Equations 13-15 and reported in Table 9.

Table 8. Ratio of **1** or **2** to chalcone **3** formed from **4** and their concentrations.

	Concentration of 1 or 2 (M)	**Concentration of 3 (M)**	**Ratio (Starting/Product)**
4a	4.48×10^{-4}	7.85×10^{-5}	5.71
4b	3.58×10^{-4}	4.41×10^{-5}	8.11
4c	2.10×10^{-4}	3.35×10^{-5}	6.27
4d	5.12×10^{-4}	8.11×10^{-5}	6.31
4e	6.95×10^{-5}	1.17×10^{-5}	5.94
4f	1.48×10^{-4}	2.59×10^{-5}	5.71

Table 9. Rate constants (k_2) for disappearance of **4** and rate constants from **4** to starting materials **1** and **2** and to chalcone **3**.

	Acetonitrile in solution (%)	**k_2 $(M^{-1}min^{-1})$**	**k from 4 to 1 and 2 $(M^{-1}min^{-1})$**	**k from 4 to 3 $(M^{-1}min^{-1})$**
4a	26[a]	2.68	2.28	0.399
4b	26	24.8	22.1	2.72
4c	60	24.0	20.7	3.30
4d	70	11.9	10.3	1.63
4e	70	19.2	16.4	2.77
4f	60	36.3	30.9	5.41

[a] The salt concentration 0.21M was used to observe disappearance of **4a**, which was at least 10 times greater salt concentration used than in **4b-f**.

IV. DISCUSSION

Rate-limiting step of chalcone formation in dehydration process

In order to complete the mechanism of chalcone formation, it is necessary to find the rate-limiting step of chalcone formation. The mechanism of chalcone formation (Scheme 2) has previously been discussed in introduction, where the first three steps of the mechanism including Deprotonation 1, Addition, and Proton Equilibration steps have been eliminated to be rate-limiting step of the reaction. This leaves us with the dehydration as the rate-limiting step in chalcone mechanism. There are two steps in dehydration process shown in Scheme 4 including Deprotonation 2, the removal of proton and forming an enolate, and Elimination, the leaving of hydroxide group and forming a double bond.

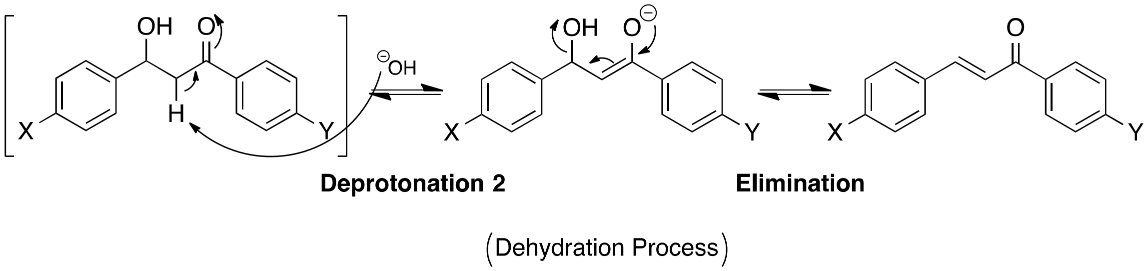

Scheme 4. Dehydration process of chalcone formation.

Meaning of results for isotope effect (k_D/k_H)

We utilized UV spectrophotometry to help us approach the answer by obtaining the third order forward rate constants in H_2O and D_2O, k_H and k_D. The isotope effect (k_D/k_H) for each **3** in Table 6 and 7 was used to determine the rate-limiting step of formation of each **3**. According to the results, the values of isotope effect for all **3** were greater than 1, which means the third order forward rate constants in D_2O are faster than the ones in H_2O ($k_D > k_H$). The isotope effect for each **3** is expected to be similar despite whether it contains an electron-withdrawing or electron-donating group. In Scheme 4, transition states in the dehydration process for both Deprotonation 2 and Elimination have the presence of negative charges, so an electron-withdrawing or electron-donating group will stabilize or destabilize both transition states instead of just one of them, making the solvent isotope effect on the rate of formation of each substituted **3** similar. The isotope effect for each **3** provides us a big clue to determine the rate-limiting step of the reaction.

Breakage of C-H bond vs. C-D bond in Deprotonation 2 step

When the kinetic experiment of formation of **3** was run in D_2O, **2** exchanged its hydrogen (H) for deuterium (D) and the intermediate **4** of the reaction transformed to the structure shown in Scheme 5.

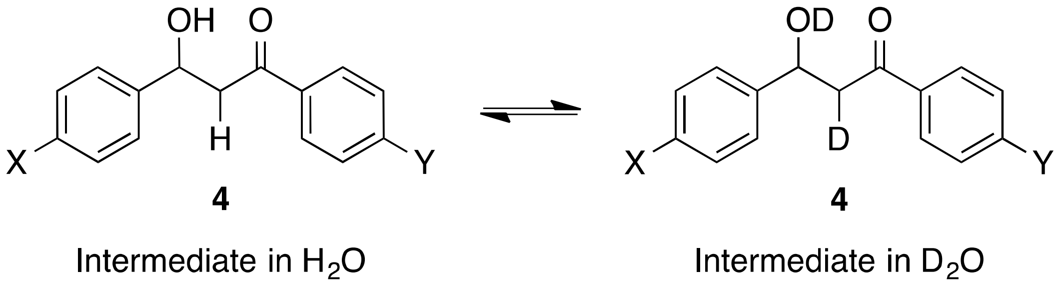

Scheme 5. Intermediate of chalcone formation in H_2O and D_2O.

We can compare the carbon hydrogen bond (C-H) and carbon deuterium bond (C-D) at α carbon position in **4** to figure out the rate-limiting step. If Deprotonation 2, the removal of proton and forming an enolate, is the rate-limiting step of the reaction, the third order forward rate constants in D_2O (k_D) is expected to be slower than the ones in H_2O (k_H) because it is harder to break a C-D bond than to break a C-H bond due to vibrational frequency and zero-point energy. The difference in vibrational frequencies of protium and deuterium will cause this deceleration when the reaction is in D_2O. However, results of k_H, k_D, and isotope effects for formation of all **3** in Table 6 and 7 show that $k_D > k_H$, indicating Deprotonation 2 step can not be the rate-limiting step of the reaction.

The rate-limiting step of chalcone formation

We have so far eliminated Deprotonation 1, Addition, and Proton Equilibration steps simply because they are fast. Rate-limiting step is the slowest step of the entire reaction that the whole reaction rate basically depends on it. According to isotope effect for each **3** obtained in Table 6 and 7 and discussion of breaking of C-H bond vs. C-D bond, Deprotonation 2 in dehydration process is eliminated as rate-limiting of chalcone formation. Using process of elimination, we conclude that the rate-limiting step of formation of **3** is Elimination (Scheme 6), the step that involves the leaving of hydroxide group and forming a double bond, in dehydration process.

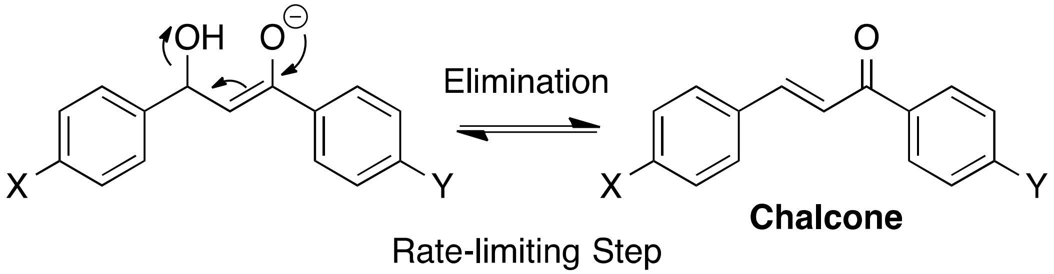

Scheme 6. Rate-limiting step of chalcone formation via aldol condensation.

Explanation for $k_D > k_H$ in chalcone formation

Previously, we have discussed that the rate in D_2O will be slower than that in H_2O ($k_D < k_H$) if Deprotonation 2 is the rate-limiting step of the reaction because it involves the breaking of C-H bond and C-D bond. Then the results showing $k_D > k_H$ suggest otherwise and lead us to reject Deprotonation 2 as rate-limiting of the reaction, leaving us with the final answer, the Elimination step. In the formation of each **3**, the third order forward rate constant in D_2O is faster than that in H_2O. This is because D_2O self ionizes less than H_2O, and the ionization constants (K_w) for H_2O and D_2O at 25°C ($K_w = [D_3O^+][OD^-] \approx 1.0 \times 10^{-15}$) ($K_w = [H_3O^+][OH^-] \approx 1.0 \times 10^{-14}$) are slightly different, which makes the $-\log K_w$ of D_2O (14.951) higher than that of H_2O (13.995) at 25°C. [25] Therefore, OD^- is more basic than OH^- and D_3O^+ is more acidic than H_3O^+. This characteristic accelerates the formation of **3** in D_2O by forming more of the enolated compound before the Elimination step.

Partitioning ratio of intermediate ketol to starting materials and to product

In Noyce's paper, he suggested that **4** reverts to **1** and **2** at a faster rate than it proceeds to **3**, indicating that the Addition step is faster than the dehydration process in the mechanism of formation of **3**. [11] This is the reason why Addition step was eliminated as rate-limiting of the reaction. The UV spectrum of **4** after reacting with base to produce **1**, **2**, and **3** showed absorbance at λ_{max} of **3** and λ of isosbestic point of **1** and **2**. The absorbances were converted to concentration using Equation 10. Since concentration formed is directly proportional to the rate constants, the concentration of either starting material and the concentration of product provide us the partitioning ratios (R) calculated with Equation 11 in Table 8, which show that how much faster **4** converted to **1** or **2** than to **3**. The results in Table 8 are consistent with Noyce's paper as each **4** reverts to its **1** and **2** faster than it converts to **3**.,

Rates from ketol intermediate to starting materials and to product

It is crucial to have a complete understanding of the rate constants from **4** to starting materials **1** and **2**, relative to the rate constant from **4** to chalcone **3**. We successfully synthesized **4a-f** to perform a series of experiments to analyze the rate constants from each **4** to its **1** and **2** and to chalcone **3**. The k_{obs} for disappearance of **4** was measured at the λ_{max} of **3** to observe appearance of **3** in **Error! Reference source not found.** using UV spectrophotometer since the half-life of the reaction is the same. Since $k_{obs} = k_2[^{-}OH]$ as described in Equation 12, the rate constant for disappearance of **4** (k_2) was calculated using the measured k_{obs} divided by [$^{-}$OH], which is equal to the sum of rate constants from **4** to **1** and **2** and to **3**. The rate constants (k_2) for disappearance of **4** can be divided into the rate constants from **4** to **1** and **2** and to chalcone **3** by plugging the determined partitioning ratio (R) in Table 9 into Equations 13-15, and all results of rate constants are reported in Table 9.

V. CONCLUSION

The kinetics of chalcone formation via aldol condensation has been studied using UV spectrophotometry. Isotope effects k_D/k_H for formation of substituted chalcones **3a**, **3b**, **3c**, **3e**, and **3f** were determined using both Guthrie's method [17]and equilibrium law listed in Equations 3-8, as reported in Tables 6 and 7 respectively. The reported isotope effects k_D/k_H for all **3** in Tables 6 and 7 are greater than 1, meaning that the rate constant of chalcone formation is faster in D_2O than in H_2O. By rejecting as rate-limiting the breakage of a C-H bond or a C-D bond in Deprotonation 2 step, Elimination step is determined to be the rate-limiting step of formation of all **3**.

According to Noyce, the ketol intermediate **4** of chalcone formation reacted with base to form **1** and **2** and to chalcone **3** simultaneously, but with faster rate at the reverse direction to **1** and **2** [13] The ketol intermediate **4** was studied using UV spectrophotometry as well to determine the partitioning ratio (R) of concentration of **1** or **2** over concentration of **3**, rate constants (k_2) for the disappearance of **4**, and separate rate constants from **4** to **1** and **2** and from **4** to **3**. The partitioning ratios (R) in Table 8 show that the results are consistent with Noyce's experiment that each **4** reverts to **1** and **2** faster than it dehydrates to **3**, which gave us evidence to eliminate Addition step as rate-limiting. The rate constants from **4** to **1** and **2** and from **4** to **3** were also evaluated and listed in Table 9 using the partitioning ratios obtained and Equations 13-15.

Different functional groups including electron-withdrawing and electron-donating group at the para position of either **1** or **2** were used to synthesize **3a-f** and **4a-f**. The isotope effects k_D/k_H of all **3** reported in Tables 6 and 7 have similar values. This is expected because both transition states of Deprotonation 2 and Elimination in the final dehydration process have the presence of negative charges in their transition states that makes the electron-withdrawing or electron-donating functional group not favoring one over another. The partitioning ratios (R) for all **4** reacted with base in Table 8 are similar to each other as well. This is expected because the ratio (R) of concentration of **1** or **2** over concentration of **3** formed from **4** doesn't vary with substituents. However, the rate constants (k_2) for the disappearance of **4** vary with substituents. The electron-withdrawing or electron-donating group will stabilize or destabilize the negative charge in the transition state respectively, making the **4b, 4c, 4e**, and **4f** that contain electron-withdrawing group such as chloro and nitro have faster rate constants from **4** to **1** and **2** and to **3** (Table 9) than the **4a** and **4b** that contain hydrogen or electron-donating group.

The mechanism of chalcone formation via aldol condensation is completed by using several substituents of **3** and **4** to determine the rate-limiting step of the reaction using isotope effect, verify that intermediate **4** reverts to **1** and **2** faster than it dehydrates to chalcone **3**, and obtain the rate constants for disappearance of **4** and for both forward and reverse directions from ketol intermediate **4**. The classic aldol reaction that has been used in textbook as a model reaction for many years is now fully understood.

WORKS CITED

1. Adams, J. H. *British Patent*, 1,250,338, **1971**; *Chem. Abstr.* **1972**, *16*, 46956.

2. Fukomoto, J.; Okada, S. *German Patent*, 2,204,716, **1922**; *Chem. Abstr.* **1972**, *11*, 152515.

3. Horowitz, R. M.; Gentili, B. *U. S. Patent*, 3,890,298, **1975**; *Chem. Abstr.* **1975**, *83*, 147706.

4. Rizzi, G. P.; Neely, J. S. *German Patent*, 2,148,332, **1972**; *Chem. Abstr.* **1972**, *11*, 86777.

5. M. Delcarmen, G. Barrio, J. R. Barrio, G. Walker, A. Noveli and N. J. Leonard *J. Am. Chem. Soc.* **1973**, *95*, 4891.

6. Hercules Powder Co. *British Patent*, 873,021, **1959**; *Chem. Abstr.* **1962**, *56*, 6185.

7. Mitsubishi Petrochemical Co. Ltd *British Patent*, 1,128,090, **1968**; *Chem. Abstr.* **1968**, *69*, 97342.

8. Hayakawa, G.; Inoue, T. *British Patent*, 7,107,386, **1971**; *Chem. Abstr.* **1971**, *74*, 14332.

9. Hine, J. Physical Organic Chemistry, 2nd ed; New York, 1962; p 261.

10. Carey, F. A.; Sundberg, R. J. Advanced Organic Chemistry, Part A, 5th ed; New York, 2007; p 284-285.

11. Noyce, D. S.; Pryor, W. A.; Bottini, A. H. *J. Am. Chem. Soc.* **1955**, *77*, 1403.

12. Perrin, C. L.; Ohta, B. K.; Kuperman, J.; Liberman, J.; Erdélyi, M. *J. Am. Chem. Soc.* **2005**, *127*, 9641-9647.

13. Noyce, D. S.; Pryor, W. A. *J. Am. Chem. Soc.* **1958**, *81*, 618-620.

14. Kellogg, R. M.; Nieuwenhuijzen, J. W.; Pouwer, K.; Vries, T. R.; Broxterman, Q. B.; Grimbergen, R. F. P.; Kaptein, B.; La Crois, R. M.; Wever, E.; Zwaagstra, K.; Laan, A. C. *Synthesis* **2003**, *10*, 1626-1638.

15. Rezaie, R.; Heidary, M.; Soltani Rad, M. N.; Behrouz, S. *Chin. J. Chem.* **2011**, *29*, 1221-1226.

16. Weygand, C.; Bauer, E.; Gunther, H.; Heynemann, W. *Liebigs Ann. Chem.* **1927**, *459*, 99-122.

17. Guthrie, J. P.; Cossar, J.; Cullimore, P. A.; Kamkar, N. M.; Taylor, K. F. *Can. J. Chem.* **1983**, *61*, 2621-2626.

18. Wei, H.; Li, K.; Zhang, Q.; Jasoni, R. L.; Hu, J.; Pare, P. W. *Helv. Chim. Acta.* **2004**, *87*, 2354-2358.

19. Schopf, C.; Thierfelder, K. *Ann. Chem.* **1935**, *518*, 127.

20. Barbero, M.; Bazzi, S.; Cadamuro, S.; Dughera, S.; Magistris, C.; Smarra, A.; Venturello, P. *Org. Biomol. Chem.* **2011**, *9*, 2192-2197.

21. Nakagawa, T.; Fujisawa, H.; Nagata, Y.; Mukaiyama, T. *Bull. Chem. Soc. Jpn.* **2004**, *77*, 1555-1567.

22. Hasegawa, E. *J. Org. Chem.* **1991**, *56(4)*, 1631-1635.

23. Olmos, A.; Alix, A.; Sommer, J.; Pale, P. *Chem. -Eur. J.* **2009**, *15(42)*, 11229-11234.

24. Xie, K.; Cui, Y.; Liu, Y.; Fu, Y. *Chin. J. Chem.* **2007**, *25*, 839-842.

25. Lide, D. R. *CRC Handbook of Chemistry and Physics, 80th Ed.* Boca Raton, FL, 2005; p 1315.